JACS ARTICLES

Published on Web 06/16/2009

Aliphatic C−H Bond Activation Initiated by a (μ-η^2:η^2-Peroxo)dicopper(II) Complex in Comparison with Cumylperoxyl Radical

Takahiro Matsumoto,[†] Kei Ohkubo,[‡] Kaoru Honda,[†] Akiko Yazawa,[†] Hideki Furutachi,[†] Shuhei Fujinami,[†] Shunichi Fukuzumi,*[,‡] and Masatatsu Suzuki*[,†]

Department of Chemistry, Division of Material Sciences, Graduate School of Natural Science and Technology, Kanazawa University, Kakuma-machi, Kanazawa 920-1192, Japan, and Department of Material and Life Science, Graduate School of Engineering, Osaka University, and SORST, Japan Science and Technology Agency (JST), Suita, Osaka 565-0871, Japan

Received December 17, 2008; E-mail: fukuzumi@chem.eng.osaka-u.ac.jp; suzuki@cacheibm.s.kanazawa-u.ac.jp

Abstract: A (μ-η^2:η^2-peroxo)dicopper(II) complex, $[Cu_2(H\text{-}L)(O_2)]^{2+}$ (**1-O$_2$**), supported by the dinucleating ligand 1,3-bis[bis(6-methyl-2-pyridylmethyl)aminomethyl]benzene (H-L) is capable of initiating C−H bond activation of a variety of external aliphatic substrates (SH_n): 10-methyl-9,10-dihydroacridine ($AcrH_2$), 1,4-cyclohexadiene (1,4-CHD), 9,10-dihydroanthracene (9,10-DHA), fluorene, tetralin, toluene, and tetrahydrofuran (THF), which have C−H bond dissociation energies (BDEs) ranging from ∼75 kcal mol^{-1} for 1,4-CHD to ∼92 kcal mol^{-1} for THF. Oxidation of SH_n afforded a variety of oxidation products, such as dehydrogenation products ($SH_{(n-2)}$), hydroxylated and further-oxidized products ($SH_{(n-1)}OH$ and $SH_{(n-2)}{=}O$), dimers formed by coupling between substrates ($H_{(n-1)}S{-}SH_{(n-1)}$) and between substrate and H-L ($H\text{-}L{-}SH_{(n-1)}$). Kinetic studies of the oxidation of the substrates initiated by **1-O$_2$** in acetone at −70 °C revealed that there is a linear correlation between the logarithms of the rate constants for oxidation of the C−H bonds of the substrates and their BDEs, except for THF. The combination of this correlation and the relatively large deuterium kinetic isotope effects (KIEs), k_2^H/k_2^D (13 for 9,10-DHA, ≳29 for toluene, and ∼34 for THF at −70 °C and ∼9 for $AcrH_2$ at −94 °C) indicates that H-atom transfer (HAT) from SH_n (SD_n) is the rate-determining step. Kinetic studies of the oxidation of SH_n by cumylperoxyl radical showed a correlation similar to that observed for **1-O$_2$**, indicating that the reactivity of **1-O$_2$** is similar to that of cumylperoxyl radical. Thus, **1-O$_2$** is capable of initiating a wide range of oxidation reactions, including oxidation of aliphatic C−H bonds having BDEs from ∼75 to ∼92 kcal mol^{-1}, hydroxylation of the *m*-xylyl linker of H-L, and epoxidation of styrene (Matsumoto, T.; et al. *J. Am. Chem. Soc.* **2006**, *128*, 3874).

Introduction

Oxidation of organic substances by Cu_2/O_2 complexes such as (μ-η^2:η^2-peroxo)dicopper(II) and bis(μ-oxo)dicopper(III) species has attracted particular interest in biological systems and industrial processes. Many well-defined Cu_2/O_2 complexes have been developed using a variety of supporting ligands, and their oxidation reactions, such as intramolecular aromatic and aliphatic ligand hydroxylation as well as intermolecular arene hydroxylation, H-atom transfer (HAT), and oxo-transfer reactions have been explored extensively (Scheme 1).[1−7] Intramolecular oxidation reactions of the supporting ligands have provided a fundamental chemical basis for the reactivity of the Cu_2/O_2 complexes and their reaction mechanism. It has been shown that some (μ-η^2:η^2-peroxo)dicopper(II) complexes have an electrophilic nature capable of hydroxylating the arene groups of the supporting ligands via an electrophilic aromatic substitution mechanism[8−13] that is similar to that performed by

[†] Kanazawa University.
[‡] Osaka University and SORST.

(1) Karlin, K. D.; Zuberbühler, A. D. In *Bioinorganic Catalysis*, 2nd ed.; Reedijk, J., Bouwman, E., Eds.; Marcel Dekker: New York, 1999; pp 469−534.
(2) Solomon, E. I.; Chen, P.; Metz, M.; Lee, S.-K.; Palmer, A. E. *Angew. Chem., Int. Ed.* **2001**, *40*, 4570–4590.
(3) Itoh, S.; Fukuzumi, S. *Bull. Chem. Soc. Jpn.* **2002**, *75*, 2081–2095.
(4) Lewis, E. A.; Tolman, W. B. *Chem. Rev.* **2004**, *104*, 1047–1076.
(5) Mirica, L. M.; Ottenwaelder, X.; Stack, T. D. P. *Chem. Rev.* **2004**, *104*, 1013–1045.
(6) Hatcher, L. Q.; Karlin, K. D. *J. Biol. Inorg. Chem.* **2004**, *9*, 669–683.
(7) Itoh, S.; Fukuzumi, S. *Acc. Chem. Res.* **2007**, *40*, 592–600.
(8) (a) Karlin, K. D.; Cohen, B. I.; Jacobson, R. R.; Zubieta, J. *J. Am. Chem. Soc.* **1987**, *109*, 6194–6196. (b) Karlin, K. D.; Nasir, M. S.; Cohen, B. I.; Cruse, R. W.; Kaderli, S.; Zuberbühler, A. D. *J. Am. Chem. Soc.* **1994**, *116*, 1324–1336.
(9) Pidcock, E.; Obias, H. V.; Zhang, C. X.; Karlin, K. D.; Solomon, E. I. *J. Am. Chem. Soc.* **1998**, *120*, 7841–7847.
(10) Mahapatra, S.; Kaderli, S.; Llobet, A.; Neuhold, Y.-M.; Palanché, T.; Halfen, J. A.; Young, V. G., Jr.; Kaden, T. A.; Que, L., Jr.; Zuberbühler, A. D.; Tolman, W. B. *Inorg. Chem.* **1997**, *36*, 6343–6356.
(11) Matsumoto, T.; Furutachi, H.; Kobino, M.; Tomii, M.; Nagatomo, S.; Tosha, T.; Osako, T.; Fujinami, S.; Itoh, S.; Kitagawa, T.; Suzuki, M. *J. Am. Chem. Soc.* **2006**, *128*, 3874–3875.
(12) Matsumoto, T.; Furutachi, H.; Nagatomo, S.; Tosha, T.; Fujinami, S.; Kitagawa, T.; Suzuki, M. *J. Organomet. Chem.* **2007**, *692*, 111–121.
(13) De, A.; Mandal, S.; Mukherjee, R. *J. Inorg. Biochem.* **2008**, *102*, 1170–1189.

 10.1021/ja809822c CCC: $40.75

Scheme 1. Representative Oxidation Reactions Initiated by Cu_2/O_2 Complexes

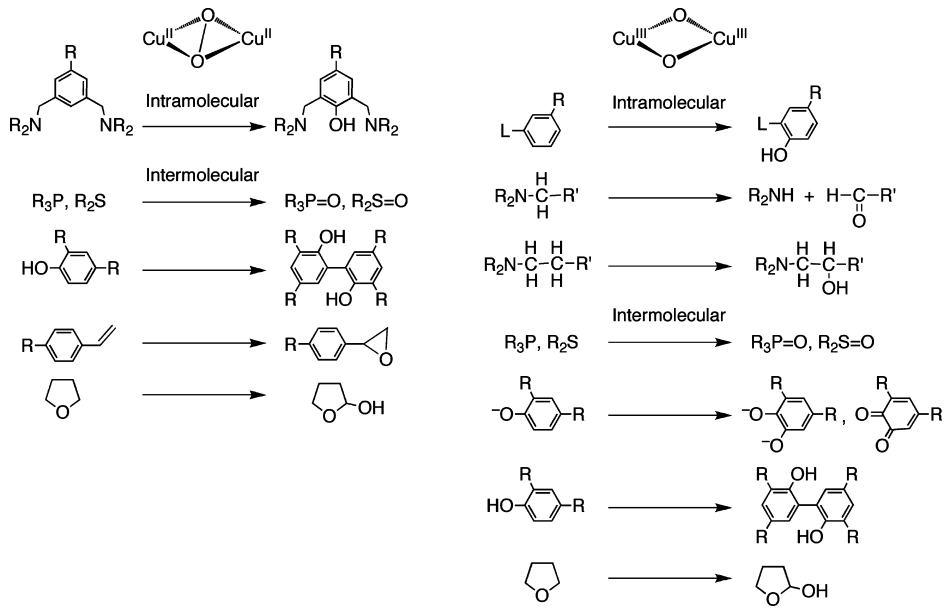

Chart 1

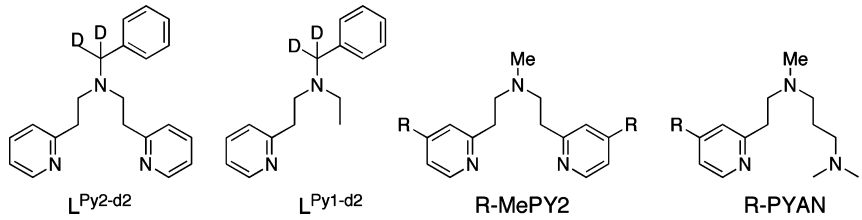

tyrosinase.[14] A similar arene hydroxylation reaction of a supporting ligand was also reported for a bis(μ-oxo)dicopper(III) complex.[15] Extensive studies of the ligand oxidation reactions by bis(μ-oxo)dicopper(III) complexes have also revealed that they tend to activate aliphatic C−H bonds of the supporting ligands.[16−21]

It has also been demonstrated that some distinct Cu_2/O_2 complexes can oxidize a variety of external substrates. Both (μ-η^2:η^2-peroxo)dicopper(II) and bis(μ-oxo)dicopper(III) complexes have been shown to oxidize external phenolates to the corresponding catechols and/or quinones.[22−26] Some kinetic studies have shown that substrate binding to the copper center is important, as observed for intramolecular hydroxylation (proximity effect), and that the reactions also proceed via an electrophilic aromatic substitution pathway. Cu_2/O_2 complexes can also oxidize phenols to produce C−C coupling dimers.[27−29] Detailed kinetic studies of the oxidation of a series of phenols having various redox potentials by (μ-η^2:η^2-peroxo)dicopper(II) and bis(μ-oxo)dicopper(III) complexes supported by the tridentate ligand $L^{Py2\text{-}d2}$ and the bidentate ligand $L^{Py1\text{-}d2}$ (Chart 1), respectively, have revealed that the reactions proceed via proton-coupled electron transfer (PCET, also known as CPET),[30] in contrast to those performed by cumylperoxyl radical (**C**), which reacts via HAT.[29]

In contrast to such oxidation of phenols, intermolecular oxidation reactions of aliphatic C−H bonds have been less well demonstrated.[31−37] It has been shown that a bis(μ-oxo)dicopper(III) complex with $L^{Py1\text{-}d2}$ is capable of oxidizing 10-methyl-9,10-dihydroacridine ($AcrH_2$) and 1,4-cyclohexadiene (1,4-

(14) Yamazaki, S.; Itoh, S. *J. Am. Chem. Soc.* **2003**, *125*, 13034–13035.
(15) Holland, P. L.; Rodgers, K. R.; Tolman, W. B. *Angew. Chem., Int. Ed.* **1999**, *38*, 1139–1142.
(16) (a) Mahapatra, S.; Halfen, J. A.; Tolman, W. B. *J. Am. Chem. Soc.* **1996**, *118*, 11575–11586. (b) Tolman, W. B. *Acc. Chem. Res.* **1997**, *30*, 227–237.
(17) Mahadevan, V.; Hou, Z.; Cole, A. P.; Root, D. E.; Lal, T. K.; Solomon, E. I.; Stack, T. D. P. *J. Am. Chem. Soc.* **1997**, *119*, 11996–11997.
(18) Itoh, S.; Nakao, H.; Berreau, L. M.; Kondo, T.; Komatsu, M.; Fukuzumi, S. *J. Am. Chem. Soc.* **1998**, *120*, 2890–2899.
(19) Itoh, S.; Taki, M.; Nakao, H.; Holland, P. L.; Tolman, W. B.; Que, L., Jr.; Fukuzumi, S. *Angew. Chem., Int. Ed.* **2000**, *39*, 398–400.
(20) Taki, M.; Teramae, S.; Nagatomo, S.; Tachi, Y.; Kitagawa, T.; Itoh, S.; Fukuzumi, S. *J. Am. Chem. Soc.* **2002**, *124*, 6367–6377.
(21) Cole, A. P.; Mahadevan, V.; Mirica, L. M.; Ottenwaelder, X.; Stack, T. D. P. *Inorg. Chem.* **2005**, *44*, 7345–7364.
(22) (a) Santagostini, L.; Gullotti, M.; Monzani, E.; Casella, L.; Dillinger, R.; Tuczek, F. *Chem.—Eur. J.* **2000**, *6*, 519–522. (b) Palavicini, S.; Granata, A.; Monzani, E.; Casella, L. *J. Am. Chem. Soc.* **2005**, *127*, 18031–18036.
(23) Itoh, S.; Kumei, H.; Taki, M.; Nagatomo, S.; Kitagawa, T.; Fukuzumi, S. *J. Am. Chem. Soc.* **2001**, *123*, 6708–6709.
(24) Mirica, L. M.; Vance, M. A.; Rudd, D. J.; Hedman, B.; Hodgson, K. O.; Solomon, E. I.; Stack, T. D. P. *J. Am. Chem. Soc.* **2002**, *124*, 9332–9333.
(25) Mirica, L. M.; Vance, M. A.; Rudd, D. J.; Hedman, B.; Hodgson, K. O.; Solomon, E. I.; Stack, T. D. P. *Science* **2005**, *308*, 1890–1892.
(26) Mirica, L. M.; Rudd, D. J.; Vance, M. A.; Solomon, E. I.; Hodgson, K. O.; Hedman, B.; Stack, T. D. P. *J. Am. Chem. Soc.* **2006**, *128*, 2654–2665.
(27) Obias, H. V.; Lin, Y.; Murthy, N. N.; Pidcock, E.; Solomon, E. I.; Ralle, M.; Blackburn, N. J.; Neuhold, Y.-M.; Zuberbühler, A. D.; Karlin, K. D. *J. Am. Chem. Soc.* **1998**, *120*, 12960–12961.
(28) Mahadevan, V.; Henson, M. J.; Solomon, E. I.; Stack, T. D. P. *J. Am. Chem. Soc.* **2000**, *122*, 10249–10250.
(29) Osako, T.; Ohkubo, K.; Taki, M.; Tachi, Y.; Fukuzumi, S.; Itoh, S. *J. Am. Chem. Soc.* **2003**, *125*, 11027–11033.

Chart 2

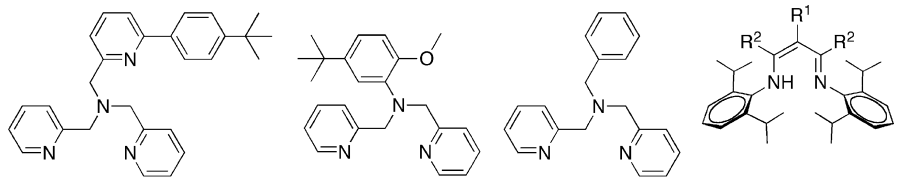

CHD) to 10-methylacridinium ion ($AcrH^+$) and benzene, respectively.[31] In this case, however, a kinetic study suggested that the reactive species was not a bis(μ-oxo)dicopper(III) species but a (μ-oxo)(μ-oxyl radical)dicopper(III) complex derived from a disproportionation reaction of two molecules of the bis(μ-oxo)dicopper(III) complex or a tetranuclear copper−oxo species.

Recently, hydroxylation of tetrahydrofuran (THF) to 2-hydroxytetrahydrofuran (2-OH-THF) by a series of (μ-η^2:η^2-peroxo)dicopper(II) complexes having tridentate ligands R-MePY2 (Chart 1) has been found,[32,33b] although they contain bis(μ-oxo)dicopper(III) species to some extent.[38] In these reactions, THF binding to the copper center is also important. Unlike THF, 9,10-dihydroanthracene (9,10-DHA), which has a much lower C−H bond dissociation energy (BDE $\approx$ 78 kcal mol^{-1})[39,40] than THF (BDE $\approx$ 92 kcal mol^{-1}),[41,42] is not oxidized by the R-MePY2 complexes. This indicates that binding of the substrate to the copper center is essential for C−H bond activation. Detailed mechanistic studies, including mechanistic probe experiments using *N*-cyclopropyl-*N*-methylaniline (CMA) and (*p*-methoxyphenyl)-2,2-dimethylpropanol (MDP), have revealed that there is a mechanistic change from PCET to HAT depending upon the redox potential ($E_{1/2}$) for a series of R-MePY2 Cu_2/O_2 complexes. Decreasing the thermodynamic driving force (i.e., $E_{1/2}$) for substrate oxidation tends to facilitate the PCET process, but a highly unfavorable ET process leads to the HAT process.[33b] Unlike the R-MePY2 complexes, a series of the closely related (μ-η^2:η^2-peroxo)dicopper(II) complexes having similar tridentate ligands R-PYAN (Chart 1), which also contain some amounts of bis(μ-oxo)dicopper(III) species, have been shown to oxidize 9,10-DHA to anthracene.[34]

Very recently, oxidation of toluene (BDE $\approx$ 88 kcal mol^{-1})[43] to benzaldehyde by a bis(μ-oxo)dicopper(III) complex bearing the tetradentate tripodal ligand 6tBP (Chart 2) has been reported.[35,36] Similar oxidations of toluene initiated by a (μ-1,2-peroxo)dicopper(II) complex with the anisole-containing tetradentate tripodal ligand ^{O}L and a bis(μ-oxo)dicopper(III) complex having the tridentate ligand ^{Bz}L (Chart 2) have also been reported.[37] In the case of the (μ-1,2-peroxo)dicopper(II) complex, some other unobservable Cu_2/O_2 species, such as a bis(μ-oxo)dicopper(III) species, have also been proposed as reactive intermediate(s). In addition to these oxidation reactions, catalytic hydroxylation of cyclohexane, which has a high C−H BDE ($\sim$98 kcal mol^{-1}) has also been reported in the reaction of copper(II) complexes supported by the β-diketiminate ligands ^{R1,R2}L [R^1 = CN, NO_2; R^2 = H (Chart 2)] with H_2O_2 at room temperature, where a bis(μ-oxo)dicopper(III) species was proposed as an active species.[44] Thus, it is of particular interest to synthesize Cu_2/O_2 complexes that are reactive toward various external organic substrates that have various BDEs and cannot coordinate to the metal center.

We have previously reported that the (μ-η^2:η^2-peroxo)dicopper(II) complex $[Cu_2(H\text{-}L)(O_2)]^{2+}$ (**1-O$_2$**), supported by the dinucleating ligand 1,3-bis[bis(6-methyl-2-pyridylmethyl)aminomethyl]benzene (H-L), can hydroxylate the *m*-xylyl linker of H-L via an electrophilic aromatic substitution mechanism, as shown in Scheme 2.[11,12] **1-O$_2$** can also epoxidize styrene via electrophilic addition to the C=C bond and hydroxylate THF by HAT.[11] Although the structure of **1-O$_2$** is not exactly known, the structure of a closely related bis(μ-hydroxo)dicopper(II) complex of H-L, ($[Cu_2(H\text{-}L)(OH)_2]^{2+}$ (**1-OH**), suggests the presence of a reaction cavity around the Cu_2/O_2 core that is accessible to substrates (Scheme 3). Despite extensive studies of the reactivity of (μ-η^2:η^2-peroxo)dicopper(II) complexes, there has to date been no report on a (μ-η^2:η^2-peroxo)dicopper(II) complex that can initiate the oxidation of the aliphatic C−H bonds of external substrates having relatively large BDEs, such as toluene.

We report herein the first extensive study of **1-O$_2$**-initiated oxidation reactions of aliphatic C−H bonds of the external substrates $AcrH_2$, 1,4-CHD, 9,10-DHA, fluorene, tetralin, toluene, and THF, which have C−H BDEs ranging from $\sim$75

(30) Although the terminology of PCET, CPET, and HAT is a matter of discussion, in this work PCET (also referred to as CPET) and HAT are used as proposed in the following papers: (a) Mayer, J. M. *Annu. Rev. Phys. Chem.* **2004**, *55*, 363–390. (b) Mayer, J. M.; Rhile, I. J.; Larsen, F. B.; Mader, E. A.; Markle, T. F.; DiPasquale, A. G. *Photosynth. Res.* **2006**, *87*, 3–20. (c) Costentin, C.; Evans, D. H.; Robert, M.; Savéant, J.-M.; Singh, P. S. *J. Am. Chem. Soc.* **2005**, *127*, 12490–12491. (d) SI in: Manner, V. W.; DiPasquale, A. G.; Mayer, J. M. *J. Am. Chem. Soc.* **2008**, *130*, 7210–7211. (e) Huynh, M. H. V.; Meyer, T. J. *Chem. Rev.* **2007**, *107*, 5004–5064.
(31) Taki, M.; Itoh, S.; Fukuzumi, S. *J. Am. Chem. Soc.* **2001**, *123*, 6203–6204.
(32) Zhang, C. X.; Liang, H.-C.; Kim, E.-i.; Shearer, J.; Helton, M. E.; Kim, E.; Kaderli, S.; Incarvito, C. D.; Zuberbühler, A. D.; Rheingold, A. L.; Karlin, K. D. *J. Am. Chem. Soc.* **2003**, *125*, 634–635.
(33) (a) Shearer, J.; Zhang, C. X.; Hatcher, L. Q.; Karlin, K. D. *J. Am. Chem. Soc.* **2003**, *125*, 12670–12671. (b) Shearer, J.; Zhang, C. X.; Zakharov, L. N.; Rheingold, A. L.; Karlin, K. D. *J. Am. Chem. Soc.* **2005**, *127*, 5469–5483.
(34) Hatcher, L. Q.; Vance, M. A.; Sarjeant, A. A. N.; Solomon, E. I.; Karlin, K. D. *Inorg. Chem.* **2006**, *45*, 3004–3013.
(35) Maiti, D.; Lucas, H. R.; Sarjeant, A. A. N.; Karlin, K. D. *J. Am. Chem. Soc.* **2007**, *129*, 6998–6999.
(36) Maiti, D.; Woertink, J. S.; Sarjeant, A. A. N.; Solomon, E. I.; Karlin, K. D. *Inorg. Chem.* **2008**, *47*, 3787–3800.
(37) Lucas, H. R.; Li, L.; Sarjeant, A. A. N.; Vance, M. A.; Solomon, E. I.; Karlin, K. D. *J. Am. Chem. Soc.* **2009**, *131*, 3230–3245.
(38) Pidcock, E.; DeBeer, S.; Obias, H. V.; Hedman, B.; Hodgson, K. O.; Karlin, K. D.; Solomon, E. I. *J. Am. Chem. Soc.* **1999**, *121*, 1870–1878.
(39) Bordwell, F. G.; Cheng, J.; Ji, G. Z.; Satish, A. V.; Zhang, X. *J. Am. Chem. Soc.* **1991**, *113*, 9790–9795.
(40) Stein, S. E.; Brown, R. L. *J. Am. Chem. Soc.* **1991**, *113*, 787–793.
(41) Mulder, P.; Laarhoven, L. J. J.; Wayner, D. D. M. *Acc. Chem. Res.* **1999**, *32*, 342–349.
(42) Laarhoven, L. J. J.; Mulder, P. *J. Phys. Chem. B* **1997**, *101*, 73–77.
(43) Berkowitz, J.; Ellison, G. B.; Gutman, D. *J. Phys. Chem.* **1994**, *98*, 2744–2765.
(44) Shimokawa, C.; Teraoka, J.; Tachi, Y.; Itoh, S. *J. Inorg. Biochem.* **2006**, *100*, 1118–1127.

Scheme 2. Reactivity of $[Cu_2(H\text{-}L)(O_2)]^{2+}$ (**1-O₂**)

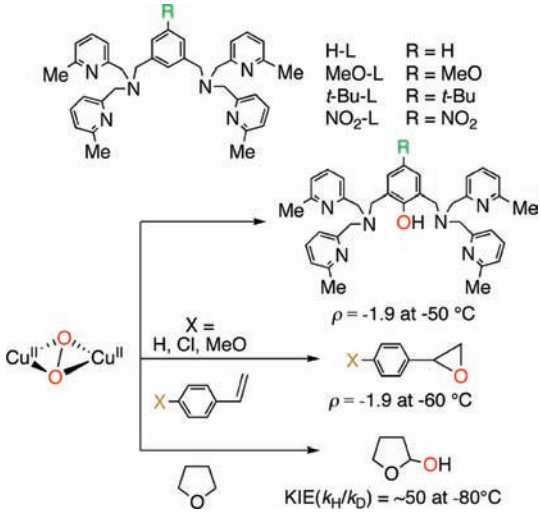

Scheme 3. Structure of $[Cu_2(H\text{-}L)(OH)_2]^{2+}$ (**1-OH**)[a]

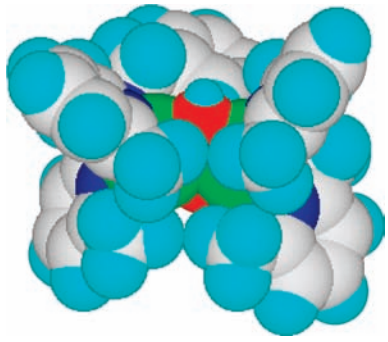

[a] Hydrogen atoms were placed at calculated positions (C−H = 1.10 Å). Color code: green, copper; red, oxygen; dark-blue, nitrogen; gray, carbon; light-blue, hydrogen.

kcal mol^{-1} for 1,4-CHD[41,45] to ∼92 kcal mol^{-1} for THF.[41,42] We also studied the reactivity of cumylperoxyl radical (**C**) toward this same series of substrates and found a striking similarity between the reactivities of **1-O₂** and **C** toward aliphatic C−H bond activation of the external substrates. The present study provides valuable mechanistic insights into C−H bond activation initiated by "Cu_2O_2" species.

Experimental Section

Materials. Acetone used in the kinetics measurements was dried over 4 Å molecular sieves and distilled under N_2 before use. For electrospray ionization−time of flight mass spectrometry (ESI−TOF/MS) measurements, spectrophotometric-grade acetone (Sigma-Aldrich) was used without further purification. 1,4-CHD was dried over CaH_2 and distilled under vacuum. 9,10-DHA, 9,10-DHA-d_4, and fluorene were recrystallized three times from EtOH under N_2. Tetralin was purified by washing with concentrated H_2SO_4 (20 times), water (three times), 10% $NaHCO_3$ (three times), and water again (three times) and then dried over Na_2SO_4 and 4 Å molecular sieves under N_2. Toluene and toluene-d_8 were washed with cold concentrated H_2SO_4 (once), water (three times), 10% $NaHCO_3$ (three times), and water again (three times), after which they were dried over $MgSO_4$ and then distilled under N_2 in the presence of Na. $AcrH_2$,[46] [9,9′-$^2H_2$]-$AcrH_2$ ($AcrD_2$),[47] 9,10-DHA-d_4,[48] H-L, and $[Cu_2(H\text{-}L)](PF_6)_2$ (**1**)[11] were synthesized according to literature methods. All other reagents and solvents were commercially available and used without further purification.

Physical Measurements. Electronic spectra were measured with a Shimadzu Multispec-1500 photodiode array spectrometer with a Unisoku thermostatted cell holder designed for low-temperature experiments or an Otsuka Electronics MCPD-2000 photodiode array spectrometer with an Otsuka Electronics optical-fiber attachment. The temperature was controlled with the Unisoku thermostatted cell holder for the former instrument and with an EYELA PSL-1800 low-temperature pair stirrer for the latter one. ^{1}H NMR spectra were measured with a JEOL JNM-LM300 or JNM-LM400 instrument using tetramethylsilane as an internal standard. GC−MS analysis was performed on a Shimadzu GCMS-QP5050A GC−MS instrument equipped with a fused silica capillary column (100% dimethylpolysiloxane, 0.32 mm diameter × 25 m, QUADREX Corp.). ESI−TOF/MS spectra were measured using a Micromass LCT spectrometer.

Kinetics Measurements on 1-O₂. The rates of **1-O₂** decomposition in the presence of various concentrations of the external substrates 1,4-CHD, 9,10-DHA, 9,10-DHA-d_4, fluorene, tetralin, toluene, toluene-d_8, THF, and THF-d_8 in acetone at −70 °C were measured by monitoring the electronic spectral change at 351 nm using the Otsuka Electronics MCPD-2000 photodiode array spectrometer with an Otsuka Electronics optical-fiber attachment (light path length = 1 cm). Complex **1** in acetone (0.026 mM, 19.75 mL) in a three-neck flask (25 mL) at −70 °C was oxygenated by bubbling of O_2 for a few minutes to give dark-green **1-O₂**, after which O_2 was removed by gentle bubbling of N_2 for ∼20 min. Next, to the resulting solution was added a cold acetone solution (100 mM, 0.25 mL) containing 9,10-DHA at −70 °C. In the case of tetralin, toluene, and toluene-d_8, the substrate was directly added to an acetone solution of **1-O₂**; cold toluene and toluene-d_8 were quickly added by a cannulation method. The final concentrations of **1-O₂** and substrate are given in Table S1 in the Supporting Information (SI). Pseudo-first-order rate constants k_{obs} were determined by least-squares curve fitting using a microcomputer (Figures S1 and S2 and Table S1 in the SI). Plots of k_{obs} versus substrate concentration were linear (Figure S3 in the SI), yielding the rate equation $v = k_{obs}[\mathbf{1\text{-}O_2}]$, in which $k_{obs} = k_1 + k_2$[substrate], where k_1 and k_2 are the rate constants for self-decomposition (ligand hydroxylation) of **1-O₂** and substrate oxidation, respectively. The self-decomposition rate constant of **1-O₂** under the above conditions was $k_1 = (5.3 \pm 0.1) \times 10^{-5}$ s^{-1}, which is in reasonable agreement with the value 6.9×10^{-5} s^{-1} estimated from an extrapolation using the activation parameters ($\Delta H^{\ddagger}$ and $\Delta S^{\ddagger}$).[11] The reaction with toluene-d_8 in a 4.7 M toluene-d_8/acetone solution yielded a very small k_{obs} value of 2.2×10^{-5} s^{-1}, which is ∼2.5 times smaller than the self-decomposition rate constant (k_1) in acetone at −70 °C. This seems to be attributable to changes in the solvent properties in going from acetone to the ∼1:1 toluene/acetone mixture.

Decomposition rates of **1-O₂** in the presence of $AcrH_2$ and $AcrD_2$ in acetone at −94 °C were measured by monitoring the electronic spectra at 351 nm using the Shimadzu photodiode array Multispec-1500 spectrometer with 1 cm cell. Typically, **1** in acetone (0.050 mM, 3 mL) at −94 °C was oxygenated by bubbling of O_2 into an acetone solution of **1** for a few minutes, after which O_2 was removed by gentle bubbling of N_2 into the solution for ∼20 min. To the resulting solution was then added an acetone solution (63 mM, 0.050 mL) containing $AcrH_2$ or $AcrD_2$ (Figures S2 and S3 and Table S1 in the SI).

Kinetics Measurements on Cumylperoxyl Radical. Photoirradiation of an oxygen-saturated acetone solution containing di-*tert*-butyl peroxide (1.0 M) and cumene (1.0 M) with a 1000 W

(45) Burkey, T. J.; Majewski, M.; Griller, D. *J. Am. Chem. Soc.* **1986**, *108*, 2218–2221.
(46) Fukuzumi, S.; Ohkubo, K.; Tokuda, Y.; Suenobu, T. *J. Am. Chem. Soc.* **2000**, *122*, 4286–4294.
(47) Fukuzumi, T.; Tokuda, Y.; Kitano, T.; Okamoto, T.; Otera, J. *J. Am. Chem. Soc.* **1993**, *115*, 8960–8968.
(48) Goldsmith, R. C.; Jonas, R. T.; Stack, T. D. P. *J. Am. Chem. Soc.* **2002**, *124*, 83–96.

Hg lamp resulted in the formation of **C** ($g = 2.0156$), which was detected at −70 °C using electron spin resonance (ESR) spectroscopy. The g value was calibrated using an Mn^{2+} marker. When the light was cut off, the decay of the ESR intensity was recorded with time. The decay rate was accelerated by the presence of $AcrH_2$, $AcrD_2$, 1,4-CHD, 9,10-DHA, 9,10-DHA-d_4, fluorene, tetralin, toluene, toluene-d_8, THF, or THF-d_8. The rate of HAT from the external substrate (SH_n) to **C** in each case was measured by monitoring the decay of the ESR signal intensity in the presence of various concentrations of SH_n in acetone at −70 °C (−94 °C for $AcrH_2$ and $AcrD_2$) (Figures S4 and S5 in the SI). Pseudo-first-order rate constants were determined by least-squares curve fitting using a microcomputer. The first-order rate law plots [$\ln(I - I_\infty)$ versus t, where I and I_∞ are the ESR intensity at time t and the final intensity, respectively] were linear for three or more half-lives, with correlation coefficients $r > 0.99$. Plots of the pseudo-first-order rate constants against the substrate concentrations were linear (Figure S6 and Table S2 in the SI).

Oxidation of 1,4-CHD, 9,10-DHA, Fluorene, Tetralin, Toluene, and Benzyl Alcohol by 1-O_2. 1. Analysis of the SH_n Oxidation Products. Complex **1** (5 mM, 3.0 mL) in acetone at ca. −80 °C was oxygenated by bubbling of O_2 for a few minutes to give a dark-green solution of **1-O_2**, after which O_2 was removed by bubbling of N_2 for ∼20 min. To the resulting solution was added an acetone solution of SH_n [2 mL of 15 mM 1,4-CHD (2 equiv), 2 mL of 150 mM 9,10-DHA (20 equiv), 2 mL of 75 mM fluorene (10 equiv), 2 mL of 750 mM tetralin (100 equiv), 3 mL of 9.4 M toluene (∼1900 equiv), or 2 mL of 121 mM benzyl alcohol (∼15 equiv)]. After decomposition of **1-O_2** at ca. −70 °C overnight, each resulting solution was warmed to room temperature, and 10 mL of hexane was added to precipitate a green powder (designated as **Cu-P**-CHD for 1,4-CHD, **Cu-P**-DHA for 9,10-DHA, **Cu-P**-Fluorene for fluorene, **Cu-P**-Tetralin for tetralin, or **Cu-P**-Toluene for toluene). After the precipitate was removed by filtration and washed [using 3:10 (v/v) acetone/hexane mixture for toluene or benzyl alcohol or a 1:4 (v/v) acetone/hexane mixture for 9,10-DHA, fluorene, or tetralin], a 3:10 (v/v) acetone/hexane solution of 2-bromo-*m*-xylene (15 mM, 500 μL) was added to the combined filtrate and washings as an internal standard for GC−MS measurements (except in the case of fluorene). The volume of the solution was then adjusted to 25 mL by addition of 3:10 (v/v) acetone/hexane and subjected to GC−MS analysis.

The GC−MS conditions [starting temperature (holding time), heating rate (final temperature, holding time), He flow rate] and results [retention time (*m/z*, ion)] were as follows: Benzene: 50 °C (1 min), 30 °C/min, 77.6 mL s^{-1}; 0.63 min (78, M^+). Anthracene: 100 °C, 30 °C/min (220 °C), 84.8 mL s^{-1}; 3.32 min (178, M^+). Fluoren-9-ol, fluoren-9-one, and 9*H*,9′*H*-[9,9′]bifluorenyl: 80 °C (2.5 min), 5.0 °C/min (160 °C, 1 min) then 40 °C/min (300 °C, 5 min), 55.2 mL s^{-1}; 16.62 min (180, M^+) for fluoren-9-one, 16.80 min (182, M^+) for fluoren-9-ol, and 24.39 min (330, M^+) for 9*H*,9′*H*-[9,9′]bifluorenyl. 1,2,3,4-Tetrahydronaphthalen-1-ol and 1,2,3,4-tetrahydronaphthalen-1-one: 100 °C (2 min), 10 °C/min (130 °C, 1 min) then 40 °C/min (300 °C, 5 min), 55.3 mL s^{-1}; 4.33 min (148, M^+) for 1,2,3,4-tetrahydronaphthalen-1-ol and 4.60 min (146, M^+) for 1,2,3,4-tetrahydronaphthalen-1-one. Benzaldehyde, benzyl alcohol, and 1,2-diphenylethane: 40 °C (1 min), 5 °C/min (80 °C) then 40 °C/min (220 °C), 50.0 mL s^{-1}; 4.30 min (106, M^+) for benzaldehyde, 6.05 min (108, M^+) for benzyl alcohol, and 11.80 min (182, M^+) for 1,2-diphenylethane. Quantitative analyses of the oxidation products were carried out by comparison with calibration curves for authentic samples.

The yields (all based on **1-O_2**, two experiments in each case) of benzene from 1,4-CHD and anthracene from 9,10-DHA were ∼40% (41 and 39%) and ∼20% (22 and 19%), respectively. The yields of benzyl alcohol, benzaldehyde, and 1,2-diphenylethane from toluene were ∼17% (18 and 16%), ∼2% (2 and 2%), and ∼6% (7 and 6%), respectively. The yield of 1,2,3,4-tetrahydronaphthalen-1-ol from tetralin was ∼19% (19 and 20%). The yield of benzaldehyde from benzyl alcohol was ∼90% (93 and 88%). Oxidation of fluorene gave no fluoren-9-ol or fluoren-9-one, but some amount of a coupling dimer was detected and tentatively assigned on the basis of the GC−MS library and mechanistic considerations. The amount was not determined because of the lack of an authentic sample.

2. $^{18}O_2$ Labeling Experiment for Toluene Oxidation. The procedure was the same as that for the $^{16}O_2$ experiment except for the use of $^{18}O_2$ (95%). The content of ^{18}O in benzyl alcohol was ∼95% [^{18}O-benzyl alcohol *m/z* (relative intensity): 110 (63, M^+), 79 (100), 51 (34)]. The content of ^{18}O in benzaldehyde was ∼40% [^{18}O-benzaldehyde *m/z* (relative intensity): 108 (34, $M^+(^{18}O)$), 106 (55, $M^+(^{16}O)$), 77 (100), 51 (64)]. The oxygen of ^{18}O-benzaldehyde was easily exchanged by adventitious $H_2{}^{16}O$, which was confirmed by the reaction of ^{16}O-benzaldehyde with $H_2{}^{18}O$.

3. Analysis of the Green Powders (Cu-P-SH_n). The green powders obtained in the above oxidation reactions of SH_n (**Cu-P**-CHD, **Cu-P**-DHA, **Cu-P**-Fluorene, **Cu-P**-Tetralin, and **Cu-P**-Toluene) were subjected to ESI−TOF/MS measurements. All of the ESI−TOF/MS spectra of acetone solutions of the green powders suggested the presence of $[Cu_2(H\text{-}L)(OH)_2]^{2+}$, $[Cu_2(H\text{-}L)(OH)(OCH_3)]^{2+}$, and complexes involving coupling dimers of H-L and SH_{n-1} (H-L−$SH_{(n-1)}$, designated as H-L-CHD, H-L-DHA, H-L-Fluorene, H-L-Tetralin, and H-L-Toluene, respectively), together with $[Cu_2(H\text{-}L\text{-}O)(OH)]^{2+}$ (where H-L-O is hydroxylated ligand H-L) and some unidentified species in some cases (see below). The presence of $[Cu_2(H\text{-}L)(OH)(OCH_3)]^{2+}$ was due to methanol present as an impurity in the spectrophotometric-grade acetone used.

4. Ligand-Recovery Experiments and Identification of H-L−$SH_{(n-1)}$. We also tried ligand-recovery experiments for the oxidations of 9,10-DHA and toluene. A green powder (**Cu-P**-Toluene) was dissolved in CH_3CN, and the solution was evaporated under a reduced pressure to afford a green oily product, to which $CHCl_3$ (20 mL) and concentrated aqueous ammonia (20 mL) were added with stirring. Organic compounds were extracted with $CHCl_3$ (3 × 20 mL). The combined extracts were dried over Na_2SO_4, and $CHCl_3$ was removed by evaporation under reduced pressure to give a yellow oil. ESI−TOF/MS of an acetone solution of the oil revealed the presence of a coupling dimer of H-L and SH_n (H-L−$SH_{(n-1)}$). ESI−TOF/MS (acetone solution containing a small amount of formic acid) *m/z* (relative intensity): H-L-Toluene: 324.2 (56) [M + 2H]$^{2+}$, 647.3 (7) [M + H]$^+$. H-L: 279.2 (100) [M + 2H]$^{2+}$, 557.3 (24) [M + H]$^+$. Hydroxylated ligand (H-L-OH): 287.2 (19) [M + 2H]$^{2+}$, 573.3 (13) [M + H]$^+$, and some unidentified signals as shown in Figure S7 in the SI. In the case of DHA oxidation, both H-L-DHA and its oxidized species were observed, the latter of which seemed to be generated by the oxidation of H-L-DHA during the workup procedure.

H-L-Toluene was isolated by silica gel column chromatography (95:5 MeOH/$CHCl_3$). ^1H NMR ($CDCl_3$, 400 MHz, ppm): 7.52−6.89 (21H, m, xyl-H, py-H, Tol-H), 3.79−3.77 (8H, m, NCH_2py), 3.67−3.66 (4H, m, NCH_2xyl), 3.10−3.00 (4H, m, pyCH_2CH_2Tol), 2.51−2.50 (9H, m, pyCH_3) (see Figure S8a in the SI).

5. Quantitative Analysis of H-L-Toluene. The oil obtained by the above ligand-recovery experiment was dissolved in a $CDCl_3$ solution containing 2,6-dimethyl-1,4-benzoquinone (8.4 mM, 1 mL), which was added as an internal standard. The amount of H-L-Toluene was determined using ^1H NMR by comparing the integration of the ethylene group of H-L-Toluene (3.0−3.1 ppm multiplet signal) with that of 2,6-dimethyl-1,4-benzoquinone (6.5 ppm signal). Yields of H-L-Toluene were ∼19 and ∼25% for two experiments. On the basis of the ^1H NMR data, H-L-OH was hardly formed (see Figure S8b in the SI).

Results and Discussion

Oxidation of the External Substrates Initiated by 1-O_2. Self-decomposition of **1-O_2** in acetone at −70 °C in the absence of SH_n followed first-order kinetics, resulting in almost quantitative hydroxylation of the xylyl linker of H-L (Scheme 2). In the

Scheme 4

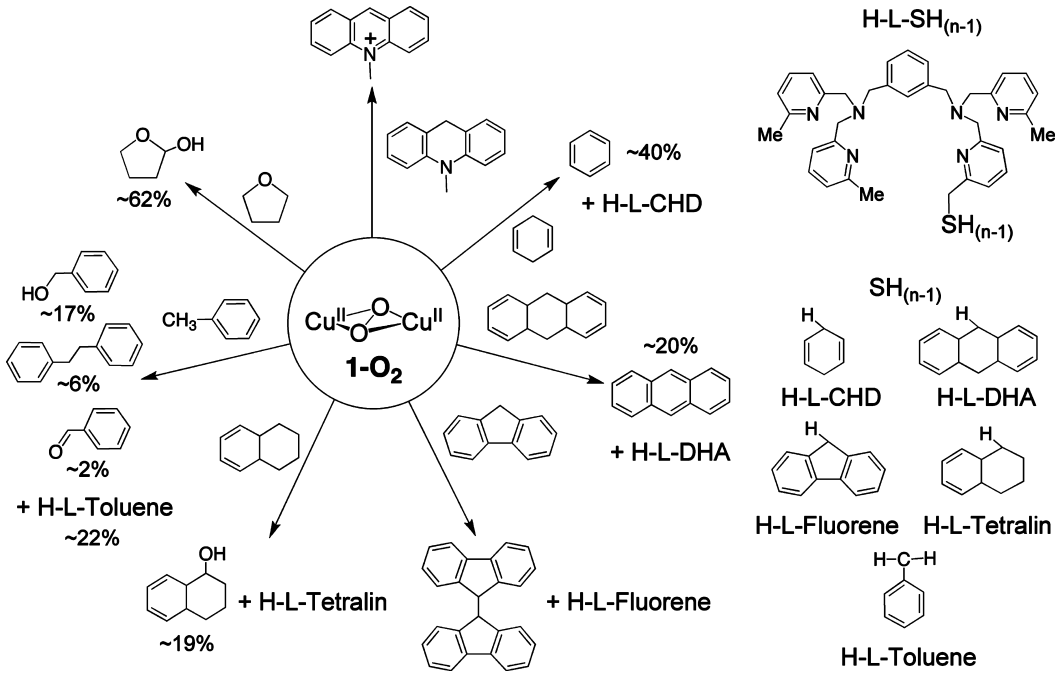

Table 1. Products of SH_n Oxidation Initiated by **1-O₂**

substrate	identified oxidation products (yield)[a]
1,4-CHD	benzene (~40%), H-L-CHD
9,10-DHA	anthracene (~20%), H-L-DHA
fluorene	9*H*,9′*H*-[9,9′]bifluorenyl, H-L-Fluorene
tetralin	1,2,3,4-tetrahydronaphthalen-1-ol (~19%), H-L-Tetralin
toluene	benzyl alcohol (~17%), benzaldehyde (~2%), 1,2-diphenylethane (~6%), H-L-Toluene (~22%)
THF	2-OH-THF (62%)
benzyl alcohol	benzaldehyde (~90%)

[a] Yields are based on **1-O₂**. Reaction conditions are given in the Experimental Section.

presence of SH_n ($AcrH_2$, 1,4-CHD, 9,10-DHA, fluorene, tetralin, toluene, THF, and benzyl alcohol), decomposition of **1-O₂** was accelerated significantly. We investigated the oxidation products of SH_n in acetone at −70 °C (with $[Cu_2] \approx 5$ mM and 2 equiv of 1,4-CHD, 20 equiv of 9,10-DHA, 10 equiv of fluorene, 100 equiv of tetralin, 100 equiv of THF, or ~1900 equiv of toluene). The oxidation products of SH_n identified in this study are shown in Scheme 4 and Table 1. Although the oxidation products have yet to be fully identified, the combined results of the analysis of the major oxidation products and the kinetic measurements (see below) provide valuable insight into the reactivity of **1-O₂**.

Oxidation of toluene gave benzyl alcohol (~17%), benzaldehyde (~2%), and 1,2-diphenylethane (~6%), which were determined by GC−MS measurement. The oxygens of benzyl alcohol and benzaldehyde came from dioxygen, which was confirmed by the $^{18}O_2$ labeling experiment. A separate experiment involving the oxidation of benzyl alcohol ($[Cu_2] \approx 5$ mM, 15 equiv of benzyl alcohol) revealed that benzyl alcohol can be oxidized to benzaldehyde in ~90% yield. The ESI−TOF/MS measurement of an acetone solution of the green powder of **Cu-P**-Toluene (see the Experimental Section) isolated after the oxidation reaction indicated the formation of a complex involving the coupling dimer of the 6-methyl radical of H-L and the methyl radical of toluene ($[Cu_2(H\text{-}L\text{-}Toluene)(OH)_2]^{2+}$ (*m*/*z* 403.1) together with $[Cu_2(H\text{-}L)(OH)_2]^{2+}$ (*m*/*z* 358.1), $[Cu_2(H\text{-}L)(OH)(OCH_3)]^{2+}$ (*m*/*z* 365.1), and $[Cu_2(H\text{-}L\text{-}O)(OH)]^{2+}$ (*m*/*z* 357.1), as shown in Figure 1a−c and Figure S9 in the SI. A ligand-recovery experiment revealed that the yield of the coupling dimer of the supporting ligand (H-L-Toluene) was ~19−25% and that of the hydroxylated ligand (H-L-OH) was negligible, as determined by ^{1}H NMR (Figure S8a,b in the SI). The total oxidation yield identified in this study was ~50%, and half of the oxidation equivalent could not be identified for the oxidation of toluene.

The oxidation of THF gave 2-OH-THF (~62%),[11] and no measurable H-L-THF was detected. The oxidations of 1,4-CHD and 9,10-DHA afforded benzene and anthracene in yields of ~40 and ~20%, respectively. ESI−TOF/MS of the corresponding powders **Cu-P**-CHD and **Cu-P**-DHA revealed the formation of coupling dimers of the methyl radical of H-L and the substrate

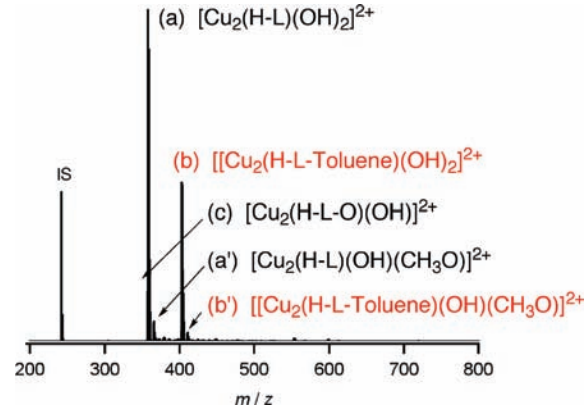

Figure 1. ESI−TOF/MS spectra of an acetone solution of a solid sample (**Cu-P**-Toluene) obtained after oxidation of toluene by **1-O₂** at −70 °C: (a) $[Cu_2(H\text{-}L)(OH)_2]^{2+}$ (*m*/*z* 358.1); (a′) $[Cu_2(H\text{-}L)(OH)(OCH_3)]^{2+}$ (*m*/*z* 365.1); (b) $[Cu_2(H\text{-}L\text{-}Toluene)(OH)_2]^{2+}$ (*m*/*z* 403.1); (b′) $[Cu_2(H\text{-}L\text{-}Toluene)(OH)(OCH_3)]^{2+}$ (*m*/*z* 410.1); (c) $[Cu_2(H\text{-}L\text{-}O)(OH)]^{2+}$ (*m*/*z* 357.1). The presence of OH and OCH_3 was confirmed via replacement by OD and OCD_3, respectively, and the presence of the methoxo species was due to a methanol impurity present in the spectrophotometric-grade acetone used. IS denotes the internal standard $[\{CH_3(CH_2)_3\}_4N^+]$ (*m*/*z* 242.2848).

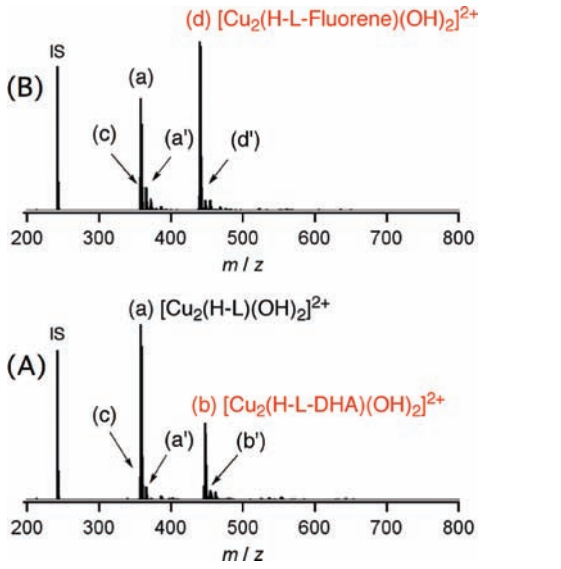

Figure 2. ESI−TOF/MS spectra of acetone solutions of the solid samples (A) **Cu-P**-DHA and (B) **Cu-P**-Fluorene obtained after oxidation of 9,10-DHA and fluorene, respectively, by **1-O$_2$** at −70 °C: (a) $[Cu_2(H\text{-}L)(OH)_2]^{2+}$ (*m*/*z* 358.1); (a′) $[Cu_2(H\text{-}L)(OH)(OCH_3)]^{2+}$ (*m*/*z* 365.1); (b) $[Cu_2(H\text{-}L\text{-}DHA)(OH)_2]^{2+}$ (*m*/*z* 447.1); (b′) $[Cu_2(H\text{-}L\text{-}DHA)(OH)(OCH_3)]^{2+}$ (*m*/*z* 454.1); (c) $[Cu_2(H\text{-}L\text{-}O)(OH)]^{2+}$ (*m*/*z* 357.1); (d) $[Cu_2(H\text{-}L\text{-}Fluorene)(OH)_2]^{2+}$ (*m*/*z* 440.1); (d′) $[Cu_2(H\text{-}L\text{-}Fluorene)(OH)(OCH_3)]^{2+}$ (*m*/*z* 447.1). IS denotes the internal standard $[\{CH_3(CH_2)_3\}_4N^+]$ (*m*/*z* 242.2848).

radicals (H-L-CHD and H-L-DHA) more or less together with H-L and H-L-OH, as shown in Figure 2A (also see Figures S10A and S11A in the SI for **Cu-P**-CHD and **Cu-P**-DHA, respectively). We tried to isolate H-L-DHA by silica gel column chromatography. However, during the workup procedure, some amount of H-L-DHA was oxidized to give an oxidized H-L-DHA, as confirmed by ESI−TOF/MS measurements. Efforts to reliably estimate their amounts by NMR measurement have been in vain to date because of the coexistence of some unidentified signals. The oxidation of fluorene gave no fluorene-9-ol, judging from the GC−MS analysis, but a coupling dimer of fluorene radicals (9*H*,9′*H*-[9,9′]bifluorenyl), which was tentatively assigned on the basis of GC−MS analysis using the GC−MS library, was found. Also, ESI−TOF/MS of **Cu-P**-Fluorene revealed the formation of a coupling dimer of H-L radical and fluorene radical (H-L-Fluorene) together with H-L and a small amount of H-L-OH (Figure 2B). The oxidation of tetralin afforded 1,2,3,4-tetrahydronaphthalen-1-ol (∼19%) and a coupling dimer of H-L radical and tetralin radical (H-L-Tetralin) (Figure S10B in the SI). Although the products have yet to be fully characterized, all of the identified products suggest the formation of C−H-bond-cleaved radicals, as indicated in Scheme 4 and Table 1.

Kinetics of the Oxidation of the C−H Bond of External Substrates Initiated by 1-O$_2$. The oxidation reactions of the external aliphatic substrates having various C−H BDEs by **1-O$_2$** were also followed by the decomposition of **1-O$_2$** monitored via the electronic spectral change at 351 nm in acetone at −70 or −94 °C. The reactions obeyed first-order kinetics under the conditions of a large excess of the substrates, and the pseudo-first-order rate constants were proportional to the concentrations of substrates (Figures 3 and 4 and Figures S1 and S2 in the SI), yielding the rate law given in eq 1:

$$v = k_{obs}[\mathbf{1\text{-}O_2}] \quad (1)$$

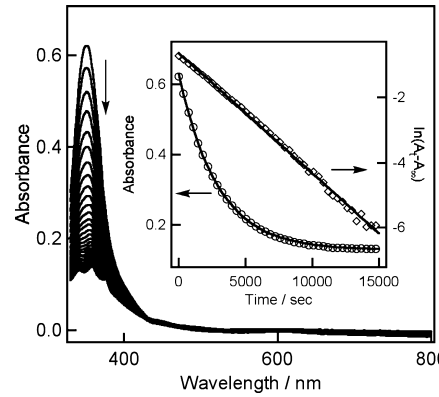

Figure 3. Electronic spectral change for the reaction of **1-O$_2$** (0.026 mM) with 9,10-DHA (1.25 mM) in acetone at −70 °C under N_2 (time interval 360 s). Inset: Decay time profile of the absorbance at 351 nm (curve) and the pseudo-first-order plot (linear plot).

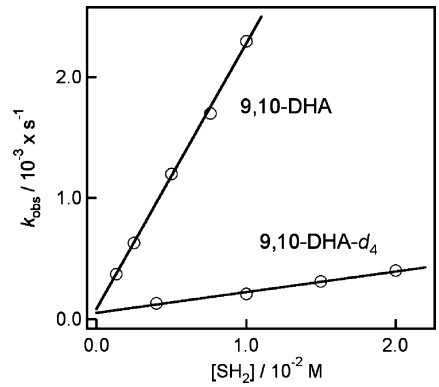

Figure 4. Plots of k_{obs} vs the concentrations of 9,10-DHA and 9,10-DHA-d_4 for the reactions with **1-O$_2$** in acetone at −70 °C.

with

$$k_{obs} = k_1 + k_2[\text{substrate}]$$

where k_{obs} is the pseudo-first-order rate constant and k_1 and k_2 are the rate constants for self-decomposition of **1-O$_2$** (hydroxylation of the xylyl linker of H-L) and oxidation of the external substrate, respectively. The self-decomposition rate constant for **1-O$_2$** (k_1) in acetone at −70 °C was determined as $(5.3 \pm 0.1) \times 10^{-5}$ s^{-1} in the absence of the substrate; this is in reasonable agreement with the value of 6.9×10^{-5} s^{-1} estimated from an extrapolation using previously reported kinetic activation parameters ($\Delta H^{\ddagger}$ and $\Delta S^{\ddagger}$).[11] The second-order rate constants (k_2) for the oxidation of SH_n were determined from the slopes of plots of k_{obs} versus SH_n concentration (Figure 4, Table 2, and Figure S3 and Table S1 in the SI). Thus, the oxidation reactions proceed through a bimolecular process.

Notably, there is a correlation between the second-order rate constants (k_2) and the BDEs of SH_n (see below). We also measured the deuterium kinetic isotope effects (KIEs), k_2^H/k_2^D, and obtained values of 13 for 9,10-DHA/9,10-DHA-d_4, >29 for toluene/toluene-d_8, and ∼34 for THF/THF-d_8 at −70 °C and ∼9 for $AcrH_2/AcrD_2$ at −94 °C. Such large KIE values indicate that the oxidation reactions proceed through the HAT process.

Kinetics of the Oxidation of the C−H Bonds of SH$_n$ by Cumylperoxyl Radical (C). Cumylperoxyl radical is known to be able to abstract a hydrogen atom from organic substrates

Table 2. Second-Order Rate Constants and Kinetic Isotope Effects (KIEs) for the Oxidations of SH_n by the (μ-η²:η²-Peroxo)dicopper(II) Complex (**1-O₂**) and $PhC(CH_3)_2OO\cdot$ (**C**) Along with Bond Dissociation Energies (BDEs) of SH_n

	1-O₂		**C**				
SH_n	k_2 (M^{-1} s^{-1})	KIE	k_2^C (M^{-1} s^{-1})	KIE	BDE (kcal mol^{-1})	refs for BDE	T (°C)
1,4-CHD	9.0 ± 0.4		3.7		75 ± 2	41, 45	−70
9,10-DHA	$(2.19 \pm 0.05) \times 10^{-1}$	13	9.6×10^{-1}	∼8	78 ± 2	39, 40	−70
9,10-DHA-d_4	$(1.7 \pm 0.1) \times 10^{-2}$		1.2×10^{-1}		−		−70
fluorene	$(2.85 \pm 0.03) \times 10^{-2}$		1.3×10^{-1}		80 ± 2	39, 40	−70
tetralin	$(2.2 \pm 0.2) \times 10^{-3}$		2.0×10^{-2}		85 ± 2	40−42	−70
toluene	$(9.9 \pm 1.1) \times 10^{-5}$	>29[b]	3.2×10^{-4}	>4	88 ± 2	43	−70
toluene-d_8	$k_{obs} \approx 2.2 \times 10^{-5}$ s^{-1}[a]		$<1 \times 10^{-4}$[c]		−		−70
THF	$(1.2 \pm 0.1) \times 10^{-2}$	∼34	1.9×10^{-3}	∼8.3	92 ± 2	41, 42	−70
THF-d_8	$(3.5 \pm 0.6) \times 10^{-4}$		2.3×10^{-4}		−		−70
$AcrH_2$	57 ± 6	∼9	2.7	∼9	73.7 ± 1	49	−94
$AcrD_2$	6.6 ± 0.9		3.0×10^{-1}		−		−94
$AcrH_2$			7.5×10	2.6	73.7 ± 1		−70
$AcrD_2$			2.9×10		−		−70

[a] The value listed is k_{obs} measured under the conditions [toluene-d_8] = 4.7 M and [**1-O₂**] = 2.6×10^{-5} M. [b] This KIE value was estimated by comparing the k_{obs} values of toluene (6.5×10^{-4} s^{-1}) and toluene-d_8 (2.2×10^{-5} s^{-1}) measured under identical conditions ([toluene] or [toluene-d_8] = 4.7 M and [**1-O₂**] = 2.6×10^{-5} M). The k_{obs} of toluene-d_8 was ∼2.5 times smaller than that of the self-decomposition of **1-O₂** [$k_1 = (5.3 \pm 0.1) \times 10^{-5}$ s^{-1}] in acetone. This seemed to be attributable to changes in the solvent properties in going from acetone to the ∼1:1 acetone/toluene mixture. [c] The value was too small to be determined accurately.

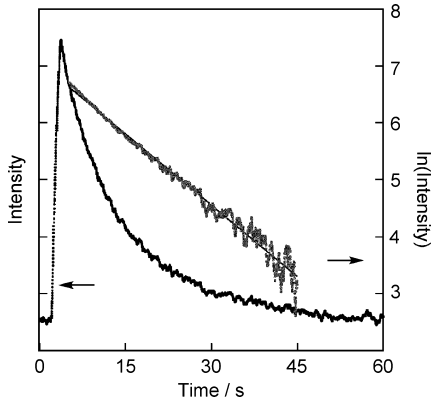

Figure 5. Decay time course of the ESR intensity due to cumylperoxyl radical in the reaction of **C** with 9,10-DHA (50 mM) in acetone at −70 °C (curve) and the pseudo-first-order plot (linear plot).

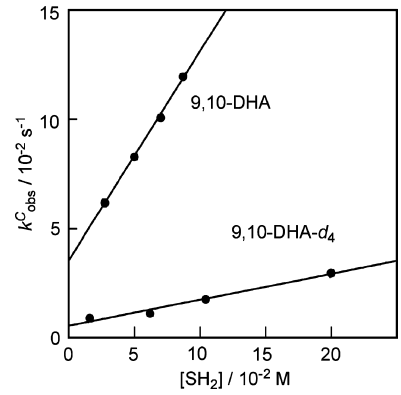

Figure 6. Plots of k_{obs}^C vs the concentrations of 9,10-DHA and 9,10-DHA-d_4 in the reactions with **C** in acetone at −70 °C.

such as phenols and *N*,*N*-dimethylanilines.[29,50] In order to compare the reactivity of **1-O₂** with that of **C**, kinetics studies of the oxidation reactions of SH_n by **C** were also performed using the same series of SH_n as employed for **1-O₂**. **C** was generated by photoirradiation of an oxygen-saturated acetone solution containing di-*tert*-butylperoxide and cumene with a 1000 W Hg lamp via a radical chain process, and **C** was readily detected by ESR spectroscopy at low temperature.[29,50] After the light was cut off, the decay rates of **C** in the reactions with SH_n were monitored by the change in the ESR intensity of **C**, as shown in Figure 5 and Figures S4 and S5 in the SI. In all cases, the decay rates were much higher than those in the absence of the substrates. The rates obeyed first-order kinetics under the conditions of a large excess of SH_n, and the pseudo-first-order rate constants (k_{obs}^C) were linearly dependent on the concentrations of SH_n, as shown in Figure 6 and Figure S6 in the SI. The second-order rate constants (k_2^C) for HAT from SH_n were determined from the slopes of the linear plots (Table 2 and Table S2 in the SI).

As in the case of the oxidation reactions initiated by **1-O₂**, a good correlation between the second-order rate constants k_2^C and the BDEs for SH_n was observed (see below). The deuterium KIEs were ∼8 for 9,10-DHA/9,10-DHA-d_4, >4 for toluene/toluene-d_8, and 8.3 for THF/THF-d_8 at −70 °C and ∼9 for $AcrH_2/AcrD_2$ at −94 °C.

Comparison of the Reactivities of 1-O₂ and C. As mentioned already, both sets of second-order rate constants, k_2 and k_2^C, correlate well with the BDEs of the C−H bonds of the substrates. For comparison of the observed second-order rate constants with the BDEs of the SH_n C−H bonds, the k_2 and k_2^C values were corrected to give k_{2c} and k_{2c}^C by dividing k_2 and k_2^C by the number of hydrogen atoms of SH_n that can be oxidized. In each case, a good linear correlation between log k_{2c} or log k_{2c}^C and the BDEs of SH_n except for THF (see below) was observed, as shown in Figure 7. Such linear correlations have been well-established for HAT reactions performed by not only organic radicals but also metal complexes,[30a,51] such as $[Mn^{VII}O_4]^-$,[52] $[Ru^{IV}(O)(bpy)_2(py)]^{2+}$,[53] $[Fe^{IV}(O)(N4Py)]^{2+}$,[54] and $[Fe^{III}(PY5)(OMe)]^{2+}$.[48] The linear correlation observed for **1-O₂**

(49) Zhu, X.-Q.; Li, H.-R.; Li, Q.; Lu, J.-Y.; Yang, Y.; Cheng, J.-P. *Chem.—Eur. J.* **2003**, *9*, 871–880.
(50) Fukuzumi, S.; Shimoosako, K.; Suenobu, T.; Watanabe, Y. *J. Am. Chem. Soc.* **2003**, *125*, 9074–9082.
(51) Mayer, J. M. *Acc. Chem. Res.* **1998**, *31*, 441–450.
(52) Gardner, K. A.; Kuehnert, L. L.; Mayer, J. M. *Inorg. Chem.* **1997**, *36*, 2069–2078.
(53) Bryant, J. R.; Mayer, J. M. *J. Am. Chem. Soc.* **2003**, *125*, 10351–10361.
(54) Kaizer, J.; Klinker, E. J.; Oh, N. Y.; Rohde, J.-U.; Song, W. J.; Stubna, A.; Kim, J.; Münck, E.; Nam, W.; Que, L., Jr. *J. Am. Chem. Soc.* **2004**, *126*, 472–473.

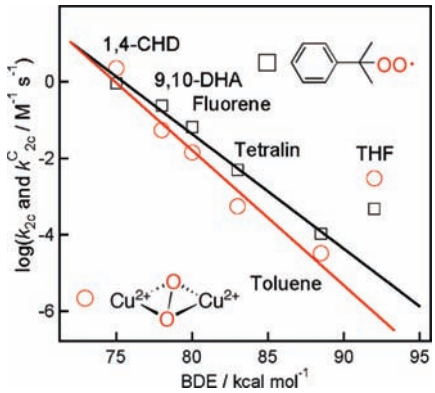

Figure 7. Plots of log k_{2c} and log k^{C}_{2c} vs SH_n BDE for the C−H bond activation of SH_n initiated by **1-O₂** (red ○) and **C** (black □) in acetone at −70 °C.

suggests that **1-O₂** has enough space around the Cu_2O_2 moiety to allow access of the external substrates irrespective of their spatial demands.

It has been shown that the rate constants for HAT reactions by a series of oxidants, including oxygen radicals (RO•) such as *tert*-butoxyl radical and *sec*-butylperoxyl radical[30a,51] and high-valent metal−oxo species such as $[Mn^{VII}O_4]^-$,[52] $[Ru^{IV}(O)(bpy)_2(py)]^{2+}$,[53] and $[Mn^{III,VI}_2(O)_2(phen)_4]^{3+}$,[55] also correlate with the BDEs of the O−H bonds formed by those oxidants. A remarkable similarity between the linear correlations observed in the oxidation reactions initiated by **1-O₂** and **C** suggests that they have a similar reactivity and that the BDEs of the O−H bonds formed by the oxidants [i.e., the BDEs of the O−H bonds of a putative $Cu^{II}(\mu\text{-OH})(\mu\text{-O})Cu^{III}$ species (see below) and cumene hydroperoxide] are comparable.

As mentioned already, the oxidation reactivity of THF with both **1-O₂** and **C** is significantly higher than that of toluene. Such higher reactivity of THF, despite the larger BDE of THF (∼92 kcal mol^{-1}) than of toluene (∼88 kcal mol^{-1}), has also been reported for HAT by *tert*-butoxyl radical, with a larger rate constant for THF (7.4×10^6 M^{-1} s^{-1}) than for toluene (1.9×10^5 M^{-1} s^{-1}) at 298 K.[56] It has been suggested that there is a pronounced stereoelectronic effect resulting in higher reactivity toward abstraction from those C−H bonds adjacent to oxygen that have a relatively small dihedral angle (∼30°) with respect to the p-type orbital on the oxygen, such as in THF.[57]

As mentioned earlier, **1-O₂** is also capable of hydroxylating the *m*-xylyl linker of H-L. The kinetic study of the hydroxylation of a series of the para-substituted *m*-xylyl linkers of $[Cu_2(R\text{-}L)(O_2)]^{2+}$ (R = MeO, *t*-Bu, H, and NO_2) showed a Hammett ρ value of −1.9 at −50 °C, indicating that the reactions proceed via an electrophilic aromatic substitution mechanism, which is consistent with the lack of a KIE by deuterium substitution at the hydroxylated position and 1,2-methyl migration upon the self-hydroxylation of the (μ-η^2:η^2-peroxo)dicopper(II) complex $[Cu_2(Me_2\text{-}L\text{-}Me)(O_2)]^{2+}$ (Me_2-L-Me = 1,3-bis[bis(6-methyl-2-pyridylmethyl)aminomethyl]-2,4,6-trimethylbenzene).[11,12] Similar ρ values have also been

Scheme 5

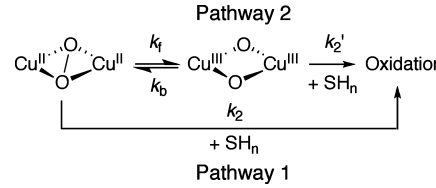

reported for the aromatic hydroxylation reactions mediated by tyrosinase (−2.4 at 25 °C)[14] and some synthetic peroxo and bis(μ-oxo)dicopper(III) complexes (ρ = −1.8 to −2.2).[8b,22b,25] In addition, **1-O₂** is also capable of oxidizing *p*-R-styrenes to the corresponding styrene oxides, where the Hammett ρ value at −60 °C was −1.9, which is the same as that for the above aromatic ligand hydroxylation. Thus, **1-O₂** can initiate a wide range of oxidation reactions.

Possible Reaction Mechanism. It has been shown that some bis(μ-oxo)dicopper(III) complexes are capable of oxidizing aliphatic C−H bonds via HAT. Although no bis(μ-oxo)dicopper(III) species was detected in the present reaction system by resonance Raman spectroscopy,[11] a small amount of bis(μ-oxo)dicopper(III) species present in a pre-equilibrium (Scheme 5) may not be excluded as a reactive species.

If this pre-equilibrium exists, two rate-determining steps are possible. In the case of a slower equilibrium between (μ-η^2:η^2-peroxo)dicopper(II) and bis(μ-oxo)dicopper(III) species and a large k_2', the rate-determining step becomes the formation of bis(μ-oxo)dicopper(III) species by O−O bond cleavage, and the observed rate constant becomes k_f. In this extreme case, the oxidation rate is not dependent upon the concentration of the substrate and a large KIE may not be observed. Itoh and co-workers have suggested that such O−O bond cleavage of the (μ-η^2:η^2-peroxo)dicopper(II) complex is involved as a rate-determining step for hydroxylation of the aliphatic C−H bond of the supporting ligand.[18] We tried to study this possibility using 10-methyl-9,10-dihydroacridine ($AcrH_2$) as an oxidation substrate, since $AcrH_2$ is much more readily oxidized than the above substrates. The kinetic study at −94 °C showed that the reaction rate was significantly accelerated ($k_2 \approx 5.7 \times 10$ M^{-1} s^{-1}) and that k_{obs} remained proportional to the concentration of $AcrH_2$. In addition, a relatively large KIE (∼9) was observed. Thus, there is no indication of a slow equilibrium between (μ-η^2:η^2-peroxo)dicopper(II) and bis(μ-oxo)dicopper(III) species in the present system. However, definitive proof of the nonexistence of a fast equilibrium between (μ-η^2:η^2-peroxo)dicopper(II) and bis(μ-oxo)dicopper(III) species has yet to be obtained. In contrast to the copper complex, we very recently found that a bis(μ-oxo)dinickel(III) complex supported by H-L can be generated in the reaction of a bis(μ-hydroxo)dinickel(II) complex with H_2O_2 and can also hydroxylate the xylyl linker of H-L.[58] Easy access to the bis(μ-oxo)dinickel(III) species by O−O bond cleavage is due to a higher d-orbital energy of the nickel complexes compared with the corresponding copper complexes.[59] It has also been found that the bis(μ-oxo)dinickel(III) complex has no reactivity toward styrene.

The oxidation of the external substrates afforded not only oxidized substrates ($SH_{(n-1)}OH$, $SH_{(n-2)}$=O, $SH_{(n-2)}$, and/or $H_{(n-1)}S-SH_{(n-1)}$) but also the coupling dimers of H-L and SH_n

(55) Larsen, A. S.; Wang, K.; Lockwood, M. A.; Rice, G. L.; Won, T.-J.; Lovell, S.; Sadílek, M.; Tureček, F.; Mayer, J. M. *J. Am. Chem. Soc.* **2002**, *124*, 10112–10123.
(56) Finn, M.; Friedline, R.; Suleman, N. K.; Wohl, C. J.; Tanko, J. M. *J. Am. Chem. Soc.* **2004**, *126*, 7578–7584.
(57) (a) Malatesta, V.; Ingold, K. U. *J. Am. Chem. Soc.* **1981**, *103*, 609–614. (b) Malatesta, V.; Scaiano, J. C. *J. Org. Chem.* **1982**, *47*, 1455–1459.
(58) Honda, K.; Cho, J.; Matsumoto, T.; Roh, J.; Furutachi, H.; Tosha, T.; Kubo, M.; Fujinami, S.; Ogura, T.; Kitagawa, T.; Suzuki, M. *Angew. Chem., Int. Ed.* **2009**, *48*, 3304–3307.
(59) Schenker, R.; Mandimutsira, B. S.; Riordan, C. G.; Brunold, T. C. *J. Am. Chem. Soc.* **2002**, *124*, 13842–13855.

Scheme 6

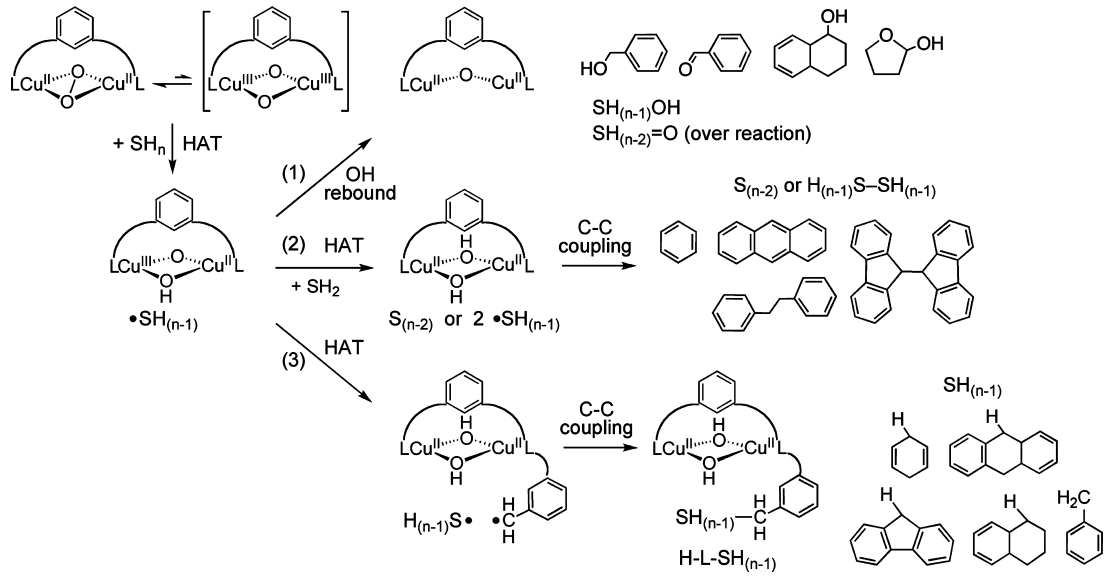

(H-L$-$SH$_{(n-1)}$), as shown in Scheme 6. The observed linear correlations of log k_{2c} and log k_{2c}^{C} with BDE in Figure 7 and the relatively large KIEs for the k_2 values clearly indicate that the rate-determining step is HAT from SH$_n$ to generate $\cdot$SH$_{(n-1)}$ radical and a putative Cu^{II}(μ-OH)(μ-O)Cu^{III}. Rebound of OH from Cu^{II}(μ-OH)(μ-O)Cu^{III} then produces SH$_{(n-1)}$OH, as shown in path (1) in Scheme 6. The formation of the coupling dimers (H$_{(n-1)}$S$-$SH$_{(n-1)}$ and H-L$-$SH$_{(n-1)}$) indicates that rebound of OH is not fast enough to preclude the coupling of $\cdot$SH$_{(n-1)}$ radicals, which affords H$_{(n-1)}$-S$-$SH$_{(n-1)}$. In the case of the formation of H-L$-$SH$_{(n-1)}$, the radical of the 6-methylpyridyl group of H-L may also be generated via HAT by $\cdot$SH$_{(n-1)}$ and/or Cu^{II}(μ-OH)(μ-O)Cu^{III}. Formation of H-L-CHD and H-L-DHA may exclude the H-atom abstraction by the radicals of 1,4-CHD and 9,10-DHA, since their BDEs ($\sim$75 to $\sim$78 kcal mol^{-1}) are significantly lower than that of the C$-$H bond of the 6-methylpyridyl group of H-L (the BDE of the C$-$H bond of 2-methylpyridine has been estimated to be $\sim$93 kcal mol^{-1}).[60] Thus, Cu^{II}(μ-OH)(μ-O)Cu^{III} seems to abstract the H atom of the 6-methylpyridyl group of H-L. The formation of such mixed-valence M^{II}(μ-OH)(μ-O)M^{III} species (M = Cu, Ni) in the oxidation reactions of (μ-η^2:η^2-peroxo)dicopper(II) complexes,[33b] bis(μ-oxo)dicopper(III) complex,[36] and bis(μ-oxo)dinickel(III) complex[61] has also been proposed. Such stepwise reactivity is in marked contrast to the reaction of **1-O$_2$** with H-L, in which the xylyl linker is selectively hydroxylated. In addition, oxidation of benzyl alcohol by **1-O$_2$** occurred smoothly with an oxidation yield of $\sim$90%, and no coupling dimer of H-L was detected.

Summary and Conclusions

The (μ-η^2:η^2-peroxo)dicopper(II) complex **1-O$_2$** [and/or Cu$_2$/O$_2$ species such as the bis(μ-oxo)dicopper(III) complex derived from **1-O$_2$**] has diverse oxidation reactivity that is capable of not only hydroxylating the xylyl linker of the supporting ligand and epoxidizing styrene but also activating the aliphatic C$-$H bond of external substrates having BDEs of 75$-$92 kcal mol^{-1}. Such diverse oxidation reactions initiated by Cu$_2$/O$_2$ species have been demonstrated for the first time in this study. Similar diverse oxidation reactions have also been demonstrated by iron(IV)$-$oxo porphyrin π-cation radicals and non-heme iron(IV)$-$oxo complexes.[62] Oxidation of the C$-$H bonds of the aliphatic substrates proceeds via a H-atom transfer process, which is evident by the linear correlation between log k_{2c} and substrate BDE and the relatively large kinetic isotope effects of k_2. Comparison of the linear correlations of log k_{2c} and log k_{2c}^{C} with the BDEs of the same series of substrates suggests that the BDE of the O$-$H bond of a putative Cu^{II}(μ-OH)(μ-O)Cu^{III} species formed after HAT from the substrates is comparable to that of cumene hydroperoxide. Although the oxidation products of the external substrates in this study have yet to be fully identified, formation of the coupling dimers of the substrate radicals (e.g., 1,2-diphenylethane), and those of the 6-methylpyridyl radical of H-L with substrate radicals (H-L$-$SH$_{(n-1)}$) indicate that the rebound of OH from Cu^{II}(μ-OH)(μ-O)Cu^{III} to the substrate radical is rather slow and that Cu^{II}(μ-OH)(μ-O)Cu^{III} is also capable of oxidizing the C$-$H bond of additional substrate and/or the 6-methylpyridyl group of H-L ligand. This reactivity of Cu^{II}(μ-OH)(μ-O)Cu^{III} is in marked contrast to the selective hydroxylation of the *m*-xylyl linker of H-L. Thus, **1-O$_2$** has a high potential for the oxidation of a variety of substrates.

Acknowledgment. This work was partly supported by Grants-in-Aid for Scientific Research, a Grant-in-Aid, and the Global COE Program "The Global Education and Research Center for Bio-Environmental Chemistry" from the Ministry of Education, Culture, Sports, Science and Technology, Japan, and by KOSEF/MEST through WCU Project (R31-2008-000-10010-0).

Supporting Information Available: Tables S1 and S2 and Figures S1$-$S11. This material is available free of charge via the Internet at http://pubs.acs.org.

JA809822C

(60) Zhao, S.-W.; Liu, L.; Fu, Y.; Guo, Q.-X. *J. Phys. Org. Chem.* **2005**, *18*, 353–367.
(61) Cho, J.; Furutachi, H.; Fujinami, S.; Ohtsu, H.; Tosha, T.; Ikeda, O.; Suzuki, A.; Nomura, M.; Uruga, T.; Tanida, H.; Kawai, T.; Tanaka, K.; Kitagawa, T.; Suzuki, M. *Inorg. Chem.* **2006**, *45*, 2873–2885.
(62) For example, see: (a) Meunier, B.; de Visser, S. P.; Shaik, S. *Chem. Rev.* **2004**, *104*, 3947–3980. (b) Nam, W. *Acc. Chem. Res.* **2007**, *40*, 522–531. (c) Song, W. J.; Ryu, Y. O.; Song, R.; Nam, W. *J. Biol. Inorg. Chem.* **2005**, *10*, 294–304.